

# Thickening Castor Oil with a Lignin-Enriched Fraction from Sugarcane Bagasse Waste via Epoxidation: A Rheological and Hydrodynamic Approach

Esperanza Cortés-Triviño,\* Concepción Valencia, and José M. Franco

Cite This: *ACS Sustainable Chem. Eng.* 2021, 9, 10503–10512

Read Online

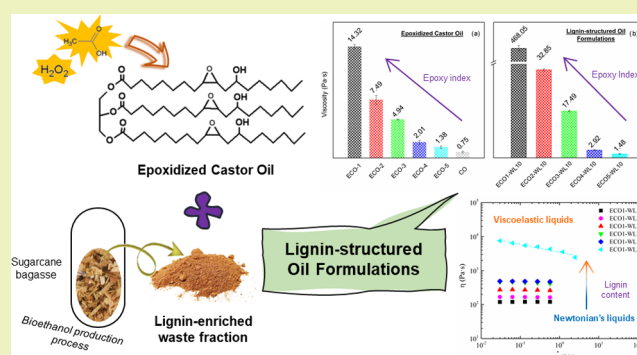
ACCESS |

Metrics &amp; More

Article Recommendations

**ABSTRACT:** Thickening vegetable oils to different extents is of great interest in the design and development of new bio-based lubricant formulations, as achieving a wide range of rheological properties is crucial to the successful replacement of petroleum-based traditional counterparts. With this aim, the influence of epoxidation degree, modified by altering the reaction conditions, on the viscous flow properties of epoxidized castor oil was investigated together with the incorporation of a lignin-enriched fraction from sugarcane bagasse waste to more extensively modify the rheological properties, thereby valorizing this waste fraction. Oil thickening was achieved by promoting the cross-linking between the epoxidized oil and the lignin-enriched fraction that enables the compatibilization of both components. Castor oil epoxidation was assessed by means of standard volumetric titration methods and infrared spectroscopy. In addition, a fully rheological characterization of both epoxidized and lignin-thickened castor oils was carried out. A hydrodynamic approach was also followed, aiming to provide an estimation of the Mark–Houwink–Sakurada parameters and relate the intrinsic viscosity with the average molecular weight of the resulting epoxidized castor oil/lignocellulosic macromolecular compounds. The chemical interaction between castor oil and the lignocellulosic material increased as the extent of epoxidation was increased, yielding a variety of rheological responses from Newtonian liquids of increasing viscosities (from around 1 to 500 Pa·s) to viscoelastic liquids.

**KEYWORDS:** epoxidized castor oil, sugarcane bagasse waste, rheology, intrinsic viscosity, molecular weight



## INTRODUCTION

Throughout the 21st century, great efforts have been made by the chemical industry to develop novel materials from biosources and/or biodegradable substances to replace the petroleum-derived raw materials currently employed,<sup>1,2</sup> aiming to reduce the impact on climate change and pollution-derived problems. This has forced the chemical industry to explore more environmentally friendly alternatives while preserving the fundamental properties and the performance of these bio-based products, as for instance in lubricant formulations. Thus, the replacement of mineral or synthetic oils, whose consumption finally implies their disposal into the environment causing severe damage to soil, water, or air,<sup>3</sup> has been widely investigated. Their substitution with vegetable oils, or some derivatives, has proven to be an effective alternative in many fields, particularly regarding the development of more sustainable lubricants.<sup>4–6</sup> However, despite many beneficial functional characteristics, like high viscosity index, good lubricity, and biodegradability, vegetable oils generally present low thermo-oxidative stability and poor fluidity at low temperatures, which restrict their end-use applications.<sup>7</sup> For

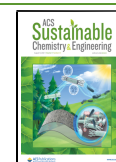
improvement of these properties, chemical modifications<sup>4,8</sup> or additives are usually required. Moreover, an important drawback associated with the use of vegetable oils as lubricants is the difficulty in obtaining a broad spectrum of viscosities or rheological properties, from low viscous liquids to semisolid or gel-like lubricants, that is, lubricating greases.<sup>9</sup>

One of the chemical modification routes widely applied to improve some of the functional properties of vegetable oils has been the epoxidation of the double bonds of their fatty acid chains, which implies the formation of an oxirane ring resulting from the acid-catalyzed peroxidation reaction between an organic acid and hydrogen peroxide, leading to the production of a percarboxylic acid.<sup>10,11</sup> Reaction variables exert an

Received: March 30, 2021

Revised: July 12, 2021

Published: July 23, 2021



important effect on the final properties of the epoxidized vegetable oil, affecting the viscous flow characteristics among others.<sup>12</sup> Thereby, vegetable oils with enhanced properties have been obtained by epoxidating their double bonds, achieving a broad range of viscosities depending on the extent of chemical modification.<sup>13</sup> Moreover, epoxides are highly reactive intermediate products since they are readily able to react with active hydrogen atom-containing compounds via nucleophilic attack, giving rise to oxirane ring opening.

On the other hand, lignocellulose is the most abundant and biorenewable material on earth, whose high production from agricultural practices has led to highly available, inexpensive, and interesting waste biosourced products.<sup>14</sup> Lignocellulosic material is composed of cellulose, hemicellulose, and lignin in proportions that depend on the source nature, with many functional groups in their structure available for chemical modifications, among which hydroxyl groups are the most relevant and feasible chemical sites.<sup>15,16</sup> These hydroxyl groups have been widely subjected to chemical reactions to produce high-value and/or end-use products with different applications.<sup>17,18</sup> Specifically, the nucleophilic attack of these hydroxyl groups on epoxy rings can be emphasized, which may give rise to more structured cross-linked networks. In previous studies,<sup>19,20</sup> different lignocellulosic fractions were functionalized with several epoxy compounds and further dispersed in vegetable oils resulting in chemical gels with potential applications as bio-based lubricating greases. An opposite approach can also be followed by inducing the epoxidation of a vegetable oil and then adding the lignocellulosic material as a viscosity modifier of the oil medium. This strategy would allow tailoring the rheological properties of vegetable oils as a function of both the oil epoxidation degree and the concentration and nature of the lignocellulosic material, which is an important requirement for lubricant applications. With this goal, this work has been focused first on the chemical modification of castor oil via epoxidation by varying the reaction conditions to modulate the viscous flow properties and obtain suitable products prone to further reactions. In addition, the thickening ability of a lignocellulosic material from sugarcane bagasse waste, mainly composed of lignin, in the epoxidized castor oil medium was evaluated to propose a new valorization pathway, and the average molecular weight of the resulting macromolecular lignocellulosic species was estimated by means of intrinsic viscosity measurements.

## EXPERIMENTAL SECTION

**Materials.** Castor oil (1.46% acidity, expressed as oleic acid) was provided by Guinama (Valencia, Spain) and further epoxidized using hydrogen peroxide (H<sub>2</sub>O<sub>2</sub>, 30 wt %), phosphoric acid (≥85 wt %), and glacial acetic acid (99.7 wt %), all of them supplied by Merck Sigma-Aldrich (St. Louis). A lignin-enriched waste fraction from the bioethanol production process involving presaccharification and simultaneous saccharification and fermentation of sugarcane bagasse was provided by CIEMAT (Madrid, Spain) and used as a thickening agent of the epoxidized castor oil. This lignocellulosic fraction contains 25.8 wt % cellulose, 3.6 wt % hemicellulose, and 56.3 wt % lignin, with an ash content of 11.4 wt %. Other common reagents and solvents were purchased from Merck Sigma-Aldrich (St. Louis).

**Epoxidation Reaction of Castor Oil.** Epoxidation of castor oil was carried out following the protocol described by Jin et al.<sup>21</sup> In brief, castor oil (60 g), glacial acetic acid (9 g), and phosphoric acid (0.6 g) were loaded into a round-bottom flask equipped with a thermometer, a reflux condenser, and a dropping funnel. The mixture was stirred until a constant temperature of 70 °C was reached. Then, different amounts of a 30 wt % H<sub>2</sub>O<sub>2</sub> solution (see Table 1) were

**Table 1. Epoxidation Degree of Castor Oil as a Function of H<sub>2</sub>O<sub>2</sub> Proportions**

epoxidized oil code	H <sub>2</sub> O <sub>2</sub> (g)	C=C/acetic acid/H <sub>2</sub> O <sub>2</sub> molar ratios <sup>a</sup>	epoxy index (mol/kg)
ECO1	48	1/0.77/24.4	2.2
ECO2	36	1/0.77/18.3	1.9
ECO3	24	1/0.77/12.2	1.6
ECO4	12	1/0.77/6.0	1.2
ECO5	6	1/0.77/3.0	0.5

<sup>a</sup>Assuming that castor oil comprises 100% ricinolein.

slowly added to the mixture, and the reaction was conducted for 4 h. According to Omonov et al.,<sup>22</sup> an excess of hydrogen peroxide is necessary to ensure that the reaction proceeds to completion. Afterward, the product was filtered, washed with distilled water, and subjected to vacuum evaporation in a rotary evaporator at 70 °C for 1 h.

The castor oil epoxidation extent was quantified according to the ISO 3001:1999 (E) standard, which is based on a titration method involving the production of nascent hydrogen bromide upon reaction with perchloric acid and tetraethylammonium bromide, determining the end-point reaction with crystal violet as an indicator.

**Preparation of Lignin-Thickened Oil Formulations.** Lignin-thickened castor oil formulations were prepared by mixing the epoxidized castor oil with the lignin-enriched fraction in the proportions given in Table 2 and then heating the mixture at 150

**Table 2. Lignin Concentrations Used for Thickening Castor Oil**

ECO	lignin-enriched waste concentrations (wt %)	formulation code
ECO1		ECO1-WL10
ECO2		ECO2-WL10
ECO3	10	ECO3-WL10
ECO4		ECO4-WL10
ECO5		ECO5-WL10
	1	ECO1-WL1
	2.5	ECO1-WL2.5
	5	ECO1-WL5
ECO1	7.5	ECO1-WL7.5
	10	ECO1-WL10
	25	ECO1-WL25

°C for 2 h in an oven followed by a homogenization treatment for 1 min at 10 000 rpm with the aid of an ULTRA-TURRAX T-25 (Ika) rotor-stator turbine. The density of the resulting lignin-thickened castor oil formulations was determined by pycnometric methods at 25 °C.

**Fourier Transform Infrared (FTIR) Spectroscopy.** FTIR spectra of both the epoxidized castor oil and the corresponding lignin-based thickened formulations were acquired in transmission mode using a FT/IR-4200 spectrometer (JASCO, Tokyo, Japan) over a wavenumber range from 400 to 4000 cm<sup>-1</sup> at 4 cm<sup>-1</sup> resolution. The device was equipped with an attenuated total reflectance (ATR) accessory provided with a monolithic diamond crystal.

**Gel Permeation Chromatography (GPC).** GPC analysis of selected lignin-thickened castor oil formulations was performed with a Waters apparatus, equipped with a high-performance liquid chromatography (HPLC) pump (Waters Mod. 1515) and two Styragel HR columns (7.8–300 mm). Measurements were done at 25 °C, and tetrahydrofuran (THF) was employed as the eluent, using a refractive index detector (Waters Mod. 2414) with a flow rate of 1.0 mL/min. Molecular weight calculations were done relatively to polystyrene standards.

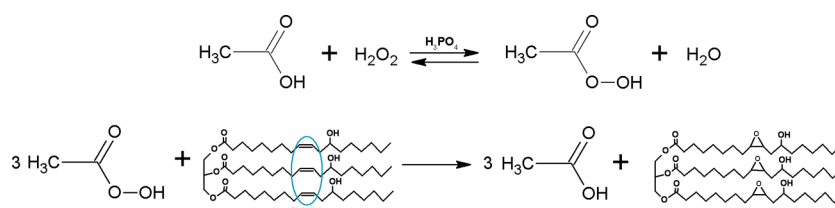


Figure 1. Castor oil epoxidation reaction.

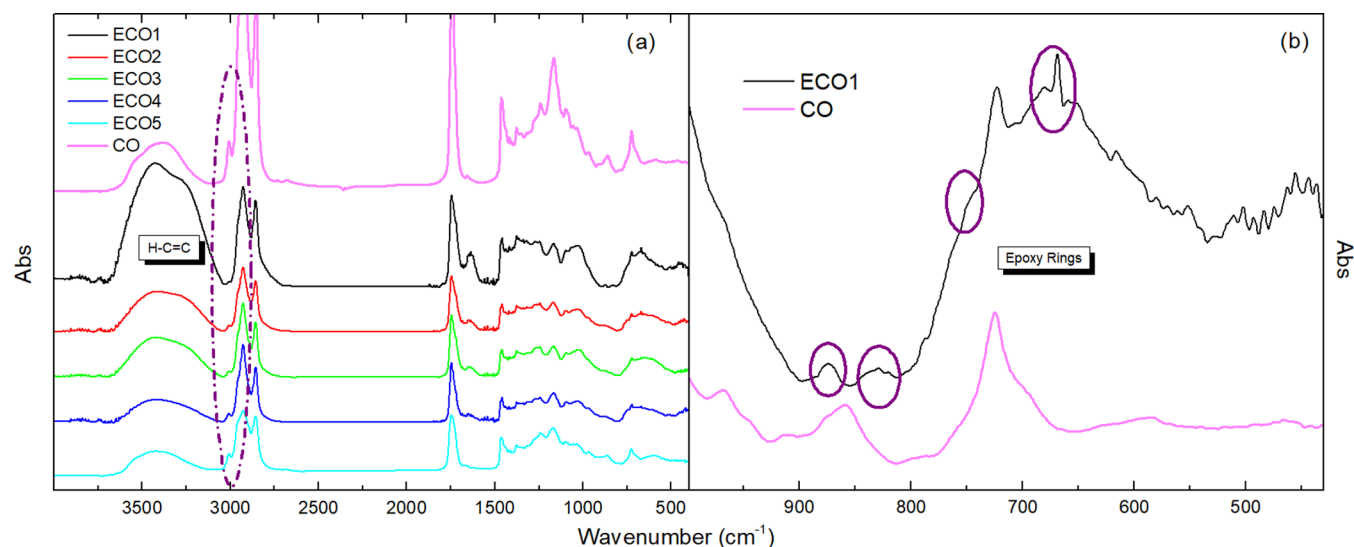


Figure 2. FTIR spectra for the different epoxidized oils.

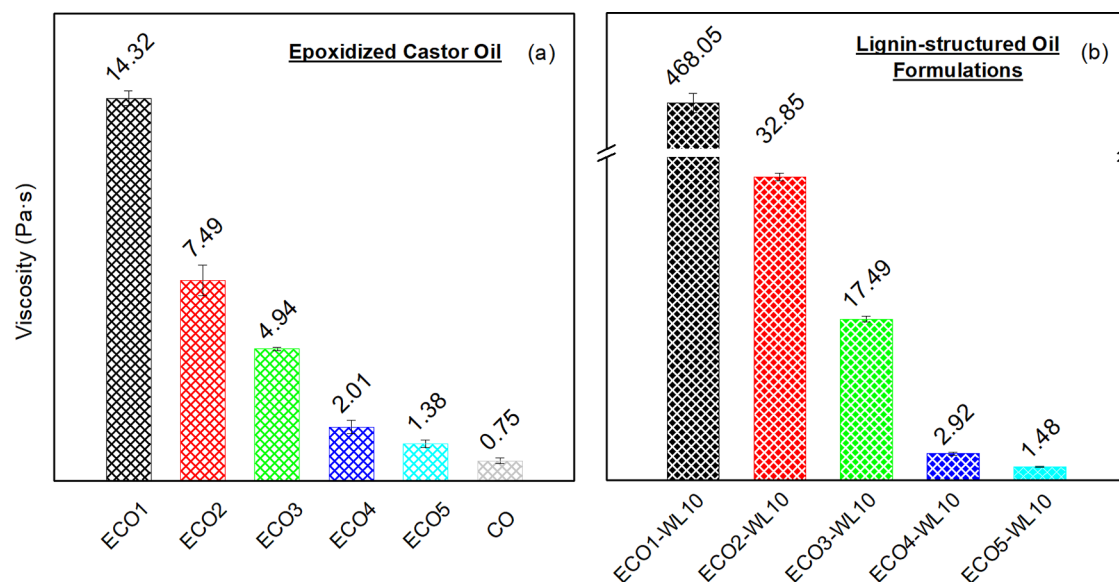


Figure 3. Viscosity values of (a) lignin-free and (b) lignin-thickened epoxidized castor oil formulations.

**Rheological Characterization.** Viscosity measurements of both raw and epoxidized castor oil samples were performed in an ARES G2 (TA Instruments) rheometer, equipped with a Peltier temperature controller, using a plate-plate geometry (50 mm, 1 mm gap). On the other hand, a Physica MCR 501 (Anton Paar, Graz, Austria) controlled-stress rheometer, also outfitted with a Peltier temperature controller, was used to rheologically characterize the lignin-thickened oil formulations, employing a serrated plate-plate geometry (25 mm, 1 mm gap) to prevent possible wall slip phenomena.<sup>23</sup> Viscous flow curves were obtained in the shear rate range of  $10^{-2}$ – $10^2$   $s^{-1}$  at different temperatures ( $-5$ – $150$  °C). Moreover, small-amplitude

oscillatory shear (SAOS) tests in the linear viscoelastic regime were carried out at 25 °C in the frequency range of 0.03–100 rad/s.

## RESULTS AND DISCUSSION

**Chemical Characterization of the Epoxidized Castor Oil.** As described elsewhere,<sup>21</sup> epoxidation of castor oil was enabled by the formation of peracetic acid, which was produced through the reaction between glacial acetic acid and hydrogen peroxide in the presence of phosphoric acid as a catalyst. The generated compound allows the epoxidation of

castor oil double bonds via donation of oxygen atoms and producing an extra amount of acetic acid (Figure 1).

Although castor oil is successfully epoxidized after 4 h of reaction, the epoxidation degree can be modulated by varying the addition of hydrogen peroxide in the functionalization reaction, maintaining the amounts of the rest of the reagents constant.<sup>24</sup> Table 1 shows the different quantities of hydrogen peroxide used to modify 60 g of castor oil, as well as the epoxidation degree quantified as the epoxy index. As can be seen, an increase of the H<sub>2</sub>O<sub>2</sub> amount used in the reaction process allowed the epoxidation of castor oil double bonds to increase as a consequence of the higher production of peracetic acid, favoring the transference of the active oxygen and therefore the formation of the epoxy ring.<sup>25</sup> On the contrary, an excess of glacial acetic acid in the mixture would trigger the opening of the newly generated epoxy rings, contributing to the reduction of the epoxy index.<sup>22</sup>

This castor oil chemical modification can also be verified by means of the infrared spectroscopy technique. Figure 2 shows the FTIR spectra of all of the epoxidized castor oil samples in comparison with the neat castor oil, where several differences can be highlighted. As previously discussed, the epoxidation of castor oil was carried out at the unsaturation sites, i.e., in the fatty acid chain double bonds, with an apparent characteristic vibration band at 3006 cm<sup>-1</sup> (Figure 2a).<sup>11,22</sup> The progressive disappearance of this characteristic band, as the H<sub>2</sub>O<sub>2</sub> amount increases, in the epoxidized samples allows confirmation of the chemical modification of castor oil double bonds and supports the different epoxidation degrees shown in Table 1. On the other hand, the presence of epoxy rings in the castor oil molecular structure can be verified by the appearance of new peaks in the wavenumber range of 900–700 cm<sup>-1</sup>, as illustrated for sample ECO1 (Figure 2b), corresponding to the stretching vibration of the C–O–C bonds in the generated epoxy groups.<sup>26,27</sup>

**Rheology of Lignin-Free and Lignin-Structured Epoxidized Castor Oils.** The influence of both the extent of epoxidation on the viscosity of modified castor oil and the further addition of 10 wt % of the lignocellulosic waste material is displayed in Figure 3. As previously discussed, the increment of hydrogen peroxide amount used in the epoxidation reaction of castor oil favored the introduction of epoxy groups into the double bonds of the fatty acid chains, which yielded a progressive increase in viscosity (Figure 3a). For example, a 10-fold viscosity increment was achieved with an epoxy index of 1.9, while a nearly 20-fold increase was obtained for the sample having an epoxy index of 2.2. The formation of the epoxy ring produces an enhanced steric hindrance as a consequence of new dipole–dipole interactions among molecules, which tend to cluster, hindering their flow and increasing the viscosity.<sup>28,29</sup> However, as reported elsewhere,<sup>30,31</sup> the Newtonian character was not altered over the range of epoxidation degrees achieved.

Besides, the addition of the lignin-enriched fraction from sugarcane bagasse waste significantly increased the viscosity values to a greater extent as the degree of epoxidation of the castor oil was increased (Figure 3b). As previously reported,<sup>19</sup> mixtures of unmodified castor oil and lignin inexorably gave rise to physically unstable dispersions, due to the lack of chemical interactions, whereas the addition of epoxidized lignin to castor oil resulted in stable gel-like dispersions as a result of the chemical reaction between epoxy and hydroxyl groups. Similarly, it is well known that castor oil epoxidation

generates new reactive sites susceptible to chemical attacks, which have been exploited for the development of novel formulations in different applications.<sup>2,32</sup> With that in mind, the addition of the lignin-enriched waste fraction to castor oil subjected to low epoxidation extents (samples ECO4 and ECO5) produced only slight changes in viscosity, resulting in stable mixtures but conditioned by a reduced number of chemical interactions between lignin hydroxyl groups and castor oil epoxy rings. On the contrary, a highly reinforced chemical structure was obtained when using the ECO1 sample, with a higher epoxy index, thus favoring the reaction between both chemical groups and leading to a strong increase in viscosity, i.e., more than a 30-fold increment.

Apart from the viscosity measurements, rheological characterization of the lignin-thickened epoxidized castor oil samples was carried out in terms of linear viscoelastic properties. Figure 4 shows the evolution of both the storage ( $G'$ ) and the loss

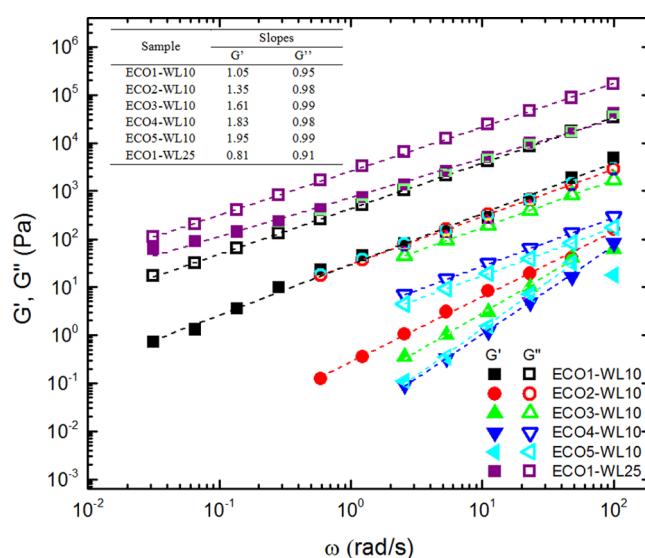
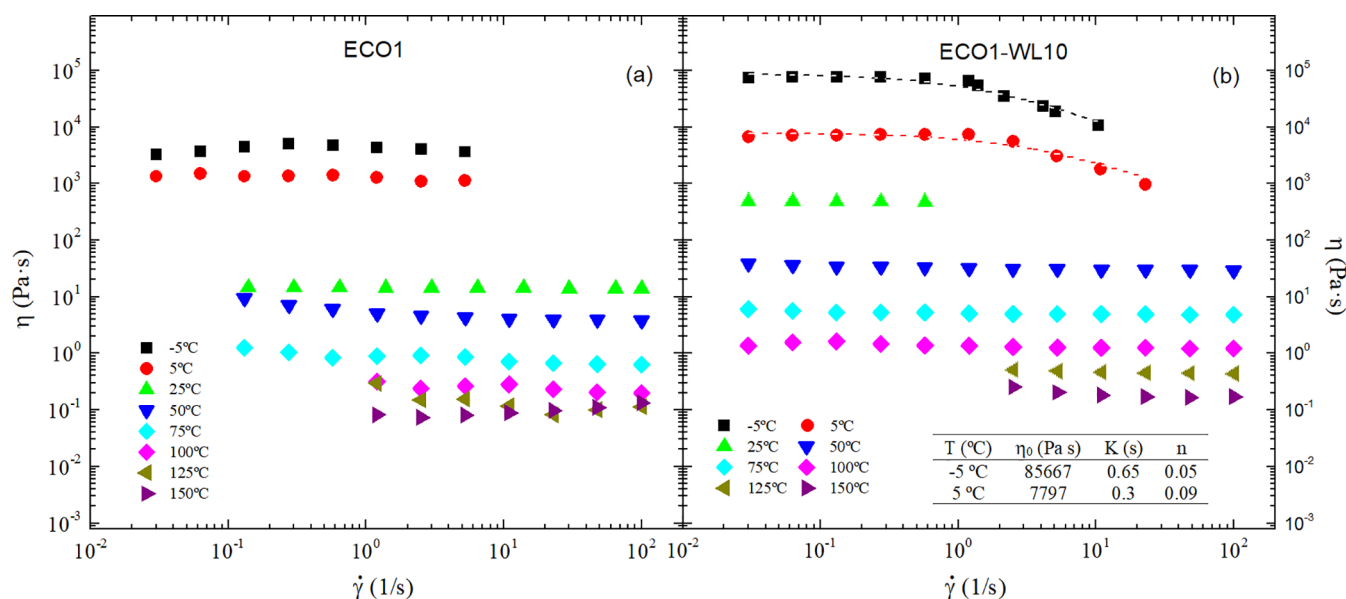


Figure 4. Viscoelastic response of lignin-structured oil formulations.

( $G''$ ) moduli with frequency, in the linear viscoelastic regime, for castor oil samples epoxidized to variable degrees and modified with 10 wt % of the lignin-enriched waste fraction. As can be seen, all samples displayed higher values of the loss modulus ( $G''$ ) than the storage modulus ( $G'$ ) in the whole frequency range studied, exhibiting a rheological response characteristic of the terminal (or flow) region of the mechanical spectrum of nonentangled viscoelastic polymeric fluids.<sup>33</sup> However, although generally these samples showed liquidlike rheological characteristics, some differences can be noticed in the slopes of the  $G'$  and  $G''$  vs frequency log–log plots (see the inset of Figure 4), depending on the epoxidation degree of castor oil (Table 2). In fact, only lignin-thickened formulations prepared with the low-epoxidized castor oil exhibited rheological responses that are strictly in accordance with the terminal flow law, i.e.,  $G'(\omega) \approx \omega^2$ ,  $G''(\omega) \approx \omega^1$ .<sup>34</sup> However, upon increasing the epoxidation degree of castor oil, a noticeable change in the slope of  $G'$  was found, and finally  $G'$  and  $G''$  attained similar frequency dependence, with both viscoelastic functions becoming closer and almost parallel when the lignin fraction was added to the most epoxidized castor oil (sample ECO1-WL10), which revealed an increased cross-linking degree.<sup>33</sup> A higher structuring level was achieved



**Figure 5.** Influence of temperature on the viscosity of (a) one selected epoxidized castor oil sample (ECO1) and (b) the lignin-thickened counterpart.

by adding 25 wt % of the lignin-enriched fraction with both viscoelastic functions becoming even closer, i.e., resulting in higher relative elasticity, and slopes for both  $G'$  and  $G''$  vs frequency plots lower than 1 in the log–log scale. Therefore, despite all samples exhibit liquidlike characteristics, the use of a highly epoxidized castor oil and lignin-enriched waste fractions allowed obtaining relatively structured formulations.

The most thickened castor oil sample (ECO1-WL10) was selected to study the influence of temperature on viscosity. Figure 5 shows the different viscosity curves as a function of the shear rate for this sample, at several temperatures (from  $-5$  to  $150$  °C) in comparison with the corresponding lignin-free epoxidized castor oil (ECO1). As can be seen, from  $25$  to  $150$  °C, both samples (ECO1 and the lignin-thickened counterpart) displayed a Newtonian behavior, decreasing the viscosity when increasing the temperature. However, a change in the rheological properties of the lignin-thickened oil was found when applying temperatures below  $25$  °C, revealing shear thinning characteristics at shear rates higher than around  $1$   $\text{s}^{-1}$ . These curves may be described according to the Cross–Williamson model ( $R^2 > 0.98$ )

$$\eta = \frac{\eta_0}{1 + (K\dot{\gamma})^m} \quad (1)$$

where  $\eta$  (Pa·s) is the dynamic viscosity,  $\eta_0$  (Pa·s) is the low-shear-rate-limiting viscosity,  $\dot{\gamma}$  is the applied shear rate ( $1/\text{s}$ ), and  $K$  (s) and  $m$  are the Cross fitting parameters,<sup>35,36</sup> with values shown in Figure 5b.

**Hydrodynamic Properties of the Lignin-Thickened Epoxidized Castor Oil.** The hydrodynamic study of the lignin-containing epoxidized castor oil was performed by modifying the concentrations of the lignin-enriched fraction from sugarcane bagasse waste in the most epoxidized castor oil sample (ECO1, see Table 2). The viscous flow curves of these systems were obtained (Figure 6) and evaluated to estimate the intrinsic viscosity properties of this lignocellulosic complex in the epoxidized castor oil. A variety of rheological responses from Newtonian liquids of increasing viscosities to non-

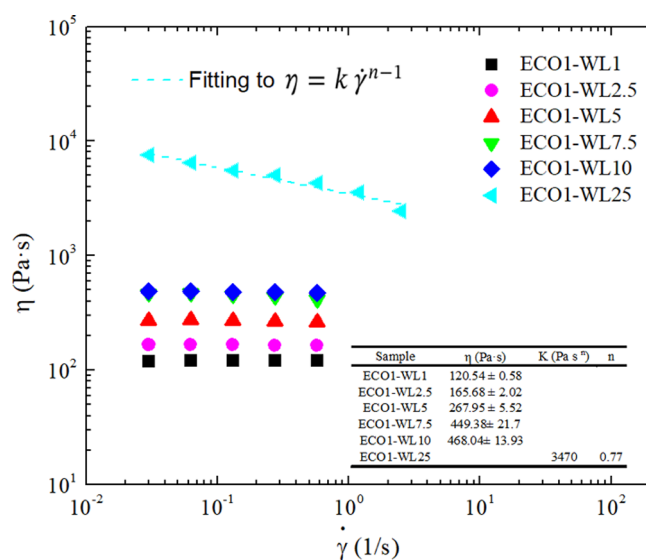


**Figure 6.** Viscosity values of the lignin-thickened castor oil as a function of the lignocellulosic fraction content.

Newtonian viscoelastic liquids were obtained by increasing the lignocellulose fraction content.

As is well known, the hydrodynamic behavior of macromolecular solutions in the diluted and semidiluted non-entangled or entangled regimes can be studied by analyzing the intrinsic viscosity, which provides information about the specific hydrodynamic volume of the chain under particular conditions (constant temperature and pressure and absence of shear) in the limit of infinite dilution. According to this, and accepting that this lignin-enriched fraction is a polymeric complex that even reacts with the epoxidized triglyceride molecules, the relationship between the reduced viscosity,  $\eta_{red}$ , and lignin-enriched fraction concentration allows determination of this parameter from the intercept with the ordinate axis in accordance with the following equations<sup>37,38</sup>

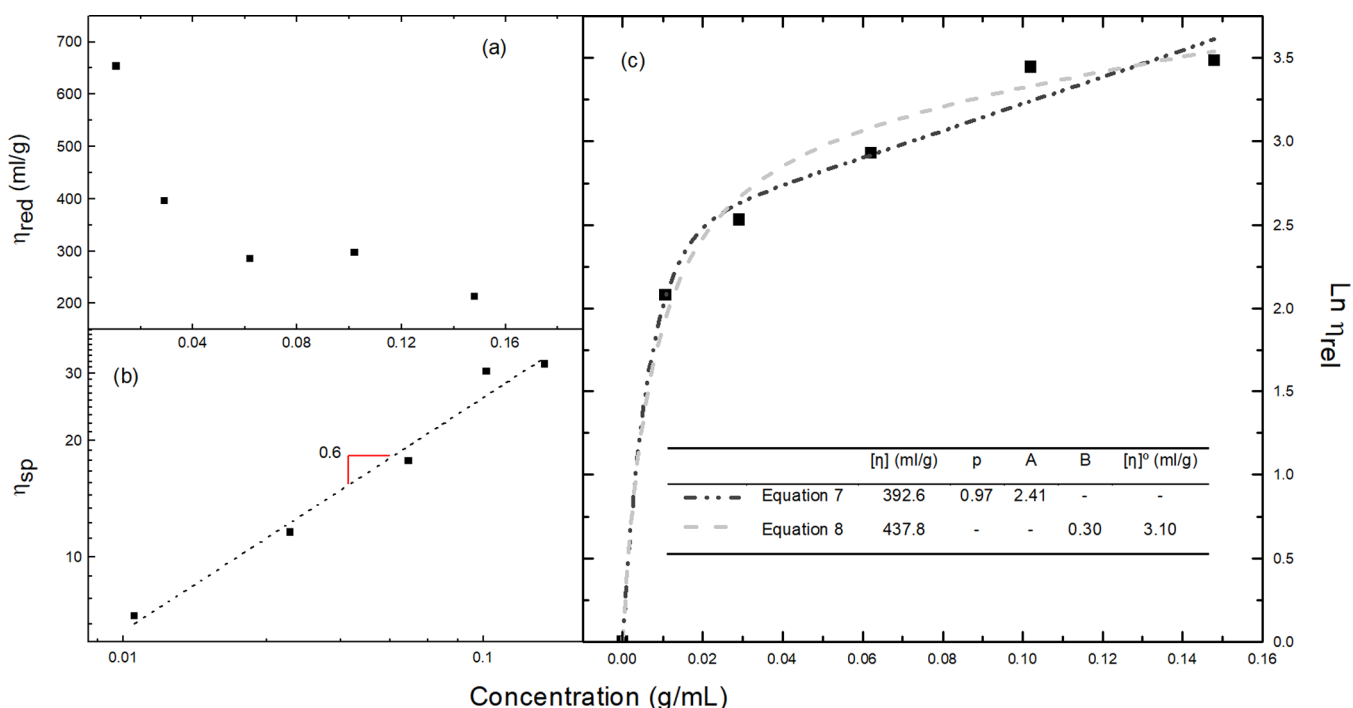


**Figure 7.** (a) Huggins plot for the lignin-structured epoxidized castor oil, (b) specific viscosity vs concentration plot, and (c) fitting the intrinsic viscosity to the Wolf model.

$$\eta_{\text{rel}} = \frac{\eta_{\text{sol}}}{\eta_{\text{ECO1}}} \quad (2)$$

$$\eta_{\text{sp}} = \frac{\eta_{\text{sol}} - \eta_{\text{ECO1}}}{\eta_{\text{ECO1}}} \quad (3)$$

$$\eta_{\text{red}} = \frac{\eta_{\text{sp}}}{c} \quad (4)$$

$$[\eta] = \lim_{c \rightarrow 0} \frac{\eta_{\text{sp}}}{c} \quad (5)$$

$$\eta_{\text{red}} = [\eta] + K_H[\eta]^2 c \quad (6)$$

where  $\eta_{\text{rel}}$  and  $\eta_{\text{sp}}$  are the relative and specific viscosities, respectively;  $\eta_{\text{sol}}$  and  $\eta_{\text{ECO1}}$  refer to the viscosities of the lignin-thickened sample and the epoxidized castor oil; and  $c$  is the polymer concentration in g/mL, which was converted from the weight fractions using the density of the blends. In this sense, Huggins expression<sup>39</sup> is the most employed procedure to determine the intrinsic viscosity  $[\eta]$  (eq 6), which usually follows a linear relationship between  $\eta_{\text{red}}$  and the concentration in the diluted and semidiluted regimes. However, a nonlinear dependence can be found in more complex systems,<sup>40,41</sup> as shown by the lignin-enriched fraction solutions in the epoxidized oil studied herein (Figure 7a), where a dramatic increase in the reduced viscosity can be noticed at low concentrations. Similar trends were observed by other authors,<sup>41,42</sup> whose results showed an unpredicted behavior in the low concentration regime. In those cases, the intrinsic viscosity was estimated according to the Wolf approach given for polyelectrolytes,<sup>43,44</sup> which can be used for other kinds of macromolecules while considering the viscosity of mixtures in terms of a state function.<sup>42</sup> In accordance with that, the intrinsic viscosity was estimated by means of the natural logarithm of the relative viscosity ( $\ln \eta_{\text{rel}}$ ) and its dependence

on the polymer concentration, via the slope of the curve at low concentrations, which can be fitted to two similar expressions

$$\ln \eta_{\text{rel}} = A(1 - e^{-pc[\eta]/A}) + (1 - p)c[\eta] \quad (7)$$

$$\ln \eta_{\text{rel}} = \frac{c[\eta] + Bc^2[\eta][\eta]^0}{1 + Bc[\eta]} \quad (8)$$

where  $A$ ,  $p$ ,  $B$ , and  $[\eta]^0$  are constants. Although both expressions proved to be applied with equal accuracy, the second one includes parameter  $B$ , which, according to the authors, provides information about the solvent–polymer and polymer–polymer interactions in the solution with the same physical meaning as  $K_H$  (the Huggins constant).<sup>42–44</sup>

As shown in Figure 7c, not very different intrinsic viscosity values were obtained from the fitting to both equations. On the other hand, values of parameter  $B$  lower than 0.5 denote a high quality of solvents, typically associated with strong polymer–solvent interactions, whereas a reduced solvent performance is usually attributed when  $B > 0.5$ .<sup>40,45</sup> The  $B$  value obtained ( $B = 0.3$ ) from the fitting is not surprising if the chemical interaction between the lignin complex and the epoxidized castor oil is considered, which logically makes this a good solvent. This fact can also be corroborated by plotting the specific viscosity as a function of concentration (Figure 7b), from which the concentration regimes and solvent–polymer interactions may be elucidated.<sup>46,47</sup> Thus, the transitions among dilute, semidilute unentangled, semidilute entangled, and concentrated regimes can be typically determined by changes in the slope of  $\eta_{\text{sp}}$  vs concentration plots at the three threshold concentrations,  $c^*$ ,  $c_e$ , and  $c^{**}$ , delimiting the different regimes.<sup>48</sup> Although only one dilution regime is apparent in Figure 7b for the lignin-thickened castor oil formulations studied, the value of the slope allows its identification. According to other authors, slopes of around 0.5–0.7 reveal a semidiluted unentangled regime with prevailing strong

interactions between polymer and solvent, again exhibiting characteristics similar to those found in polyelectrolytes.<sup>47–50</sup> In this sense, it must be again emphasized that the chemical interaction between the lignocellulosic components and the epoxidized castor oil not only generates cross-linking to some extent but also makes these biopolymers much more compatible with the castor oil. This compatibilizing effect enables the lignocellulosic components to be incorporated into the solvent, i.e., the castor oil, through covalent bonding. This fact explains why most of the lignin-thickened formulations displayed Newtonian characteristics even at relatively high concentrations (see Figure 6).

On the other hand, as well known, the intrinsic viscosity is directly correlated with the polymer molecular weight according to the Mark–Houwink–Sakurada expression<sup>51,52</sup>

$$[\eta] = KM_w^\alpha \quad (9)$$

where  $K$  and  $\alpha$  are the characteristic parameters for each polymer–solvent system. Both constants are usually estimated by means of experimental tests through the determination of the intrinsic viscosity of polymer solutions with known molecular weights.<sup>53</sup> However, the fact that the lignocellulosic waste material used in this study is composed of a mixture of different polymers, forming a complex three-dimensional structure,<sup>14</sup> together with the subsequent reaction of this complex with epoxidized triglycerides, makes the molecular weight characterization highly complicated. Instead, the Mark–Houwink–Sakurada expression has been employed in this work to provide a general estimation of the average molecular weight of this industrial lignin-enriched waste fraction obtained from sugarcane bagasse bioethanol production using reasonable assumptions of the likely values of the constants based on the data found in the literature for lignin solutions in different solvents. In this way,  $\alpha$  usually displays values from 0 to 2 depending on the characteristics of polymers in solutions. Thus,  $\alpha < 0.5$  is typical for polymers formed by rigid spheres dispersed in an ideal solvent;  $0.5 < \alpha < 0.8$  indicates the presence of good solvents with random polymer coils; and  $0.8 < \alpha < 2$  implies a rodlike structure.<sup>54</sup> Some previous studies reported  $\alpha$  values in the range of 0.2–0.3 for several isolated lignin solutions in different solvents [dimethylformamide (DMF) and dimethyl sulfoxide (DMSO)], which are typical values for polymer molecules arranged in the form of rigid spherical conformations.<sup>55–58</sup> Nevertheless, by applying these  $\alpha$  values to the intrinsic viscosity obtained from the Wolf model, excessively high molecular weight values of the order of  $10^{12}$ – $10^{18}$  g/mol are derived, which makes no physical sense. In this regard, as was previously mentioned, although this lignocellulosic waste material used in this study mostly comprises lignin, it is also composed of cellulose and hemicellulose in the proportions given in the Experimental Section. This composition, together with the fact that these different biopolymers have reacted with the epoxidized triglycerides, significantly increasing their compatibility as mentioned above, can presumably modify the conformation of the macromolecules in the castor oil medium, thus affecting the value of the Mark–Houwink–Sakurada exponent. This hypothesis is supported by the relatively high value of intrinsic viscosity estimated from eq 7, which may be related to the presence of randomly distributed polymer coils.<sup>54,59</sup> In addition, the B parameter in the Wolf expression and the specific viscosity vs concentration plot suggest very good solvent characteristics for the lignin complex with prevailing

strong polymer–solvent interactions, indeed covalent interactions. Therefore, a more feasible value in the range of 0.6–0.8 for the Mark–Houwink–Sakurada exponent might reasonably be assumed for these systems, which is also in agreement with Karmanov et al.,<sup>60</sup> who reported an  $\alpha$  value of 0.69 for isolated lignin in DMF.

Regarding  $K$  parameter, values in the range of  $10^{-3}$ – $10^{-2}$  mL/g have been reported by different authors for lignin solutions with very low intrinsic viscosity values (up to 10 mL/g).<sup>55,57</sup> However, the estimation of this parameter must be consistent with the polymer molecular weight and its corresponding intrinsic viscosity. For instance,  $K$  values of around 0.01–0.15 have been reported for cellulose and pectin in different solvents.<sup>59,61,62</sup> The average molecular weight of lignocellulosic biomass has been estimated by many researchers in previous fractionations, reporting values from 3000 to 100 000 g/mol.<sup>58,63,64</sup> This needs to be considered for their hydrodynamic characterization since, apart from lignin, lignocellulosic waste contains cellulose, hemicellulose, and other carbohydrate impurities in its composition. In this sense, Zeng et al.<sup>65</sup> determined a  $M_w$  value on the order of 4000 g/mol for a sugarcane bagasse-derived lignin fraction. On the other hand, Bezerra et al.<sup>66</sup> studied the chemical characteristics of sugarcane bagasse constituents, deducing the molecular weight for each fraction previously extracted by different methods. Thus, raw sugarcane bagasse showed average molecular weights of 160 000, 7400, and 507–3973 g/mol for cellulose, hemicellulose, and lignin fractions, respectively. As mentioned, due to the structural complexity and poor solubility of the lignin-enriched sugarcane bagasse fraction studied in most common solvents, the molecular weight characterization by GPC analysis of the raw material could not be performed satisfactorily. Nonetheless, the solubility of the lignin-thickened epoxidized castor oil formulations, for instance in THF, was higher as a consequence of the chemical interaction between the lignocellulose and the epoxidized castor oil. Although the high-molecular-weight fractions, mainly cellulose and lignocellulosic complexes, were not completely solubilized in THF, the GPC analysis allows an estimation of the average molecular weight of the soluble part of this thickened castor oil. Thus, the soluble part of sample ECO1-WL10 displayed a weight average molecular weight ( $M_w$ ) of 7400 g/mol, with a fraction of the maximum molecular weight of around 29 500 g/mol. However, it is worth mentioning that this average molecular weight data also takes into account the free triglycerides in excess and, in any case, it is an underestimated value since the nonsoluble fraction in THF, presumably corresponding to the high-molecular-weight molecules, mainly cellulose and lignin-carbohydrate complexes (LCCs), was not considered. According to these bibliographic and experimental data, and bearing in mind the chemical composition of the raw material employed in this work, a rough estimation of the average molecular weight of the resulting cross-linked castor oil-lignocellulose macromolecule might be around 15 000–40 000 g/mol, which is in agreement with Mark–Houwink–Sakurada constants in the range of  $\alpha = 0.80$ – $0.85$  and  $K = 0.05$ – $0.15$  mL/g.

## CONCLUSIONS

The extent of castor oil epoxidation was modified by varying the amount of  $H_2O_2$  used in the functionalization reaction, which allowed the viscous flow properties of the resulting epoxidized samples to be tailored. Up to 20-fold viscosity

increment was obtained for the most epoxidized castor oil samples while maintaining the Newtonian characteristics. Further, the epoxidation of castor oil led to the development of novel lignin-thickened oil formulations by promoting the nucleophilic interaction between lignocellulose hydroxyl groups and epoxy groups. A variety of rheological responses from Newtonian liquids of increasing viscosities (from around 1 to 500 Pa·s) to non-Newtonian viscoelastic liquids were obtained by modifying both the castor oil epoxidation degree and the content of the lignin-enriched fraction from sugarcane bagasse waste to be valorized.

A hydrodynamic study based on the determination of intrinsic viscosity properties by means of the Wolf expression allowed us to elucidate good solvent characteristics of the epoxidized castor oil with prevailing strong interactions between the lignocellulosic fraction and the epoxidized castor oil, proving the compatibilization of the lignin-enriched fraction and castor oil via chemical interaction. Moreover, an estimation of the Mark–Houwink–Sakurada parameters based on the GPC analysis of the soluble part of the lignin-thickened castor oil formulations and the data found in the literature provided an intrinsic viscosity-average molecular weight relationship for the resulting epoxidized castor oil/lignocellulose macromolecular compound, from which an average molecular weight on the order of 15 000–40 000 g/mol was deduced. Overall, lignin-enriched fractions from sugarcane bagasse waste can be proposed as effective thickening agents of vegetable oils via epoxidation.

## AUTHOR INFORMATION

### Corresponding Author

Esperanza Cortés-Triviño – Pro<sup>2</sup>TecS—Chemical Process and Product Technology Research Centre, Departamento de Ingeniería Química, ETSI, Campus de “El Carmen”, Universidad de Huelva, 21071 Huelva, Spain; [orcid.org/0000-0002-4880-9613](https://orcid.org/0000-0002-4880-9613); Phone: +34 959 217702; Email: [esperanza.cortes@diq.uhu.es](mailto:esperanza.cortes@diq.uhu.es)

### Authors

Concepción Valencia – Pro<sup>2</sup>TecS—Chemical Process and Product Technology Research Centre, Departamento de Ingeniería Química, ETSI, Campus de “El Carmen”, Universidad de Huelva, 21071 Huelva, Spain; [orcid.org/0000-0002-9197-4606](https://orcid.org/0000-0002-9197-4606)

José M. Franco – Pro<sup>2</sup>TecS—Chemical Process and Product Technology Research Centre, Departamento de Ingeniería Química, ETSI, Campus de “El Carmen”, Universidad de Huelva, 21071 Huelva, Spain; [orcid.org/0000-0002-3165-394X](https://orcid.org/0000-0002-3165-394X)

Complete contact information is available at: <https://pubs.acs.org/10.1021/acssuschemeng.1c02166>

### Notes

The authors declare no competing financial interest.

## ACKNOWLEDGMENTS

This work is part of a research project (RTI2018-096080-B-C21) sponsored by the MICINN-FEDER I+D+i Spanish Programme. The financial support is gratefully acknowledged. The authors are also grateful to Dr. Ignacio Ballesteros (CIEMAT—Madrid, Spain) for kindly providing the lignin-enriched waste fraction used in this study.

## REFERENCES

- (1) Figueiredo, J.; Ismael, M.; Anjo, C. M.; Duarte, A. Cellulose and Derivatives from Wood and Fibers as Renewable Sources of Raw-Materials. *Top. Curr. Chem.* **2010**, *294*, 117–128.
- (2) Sardari, A.; Alvani, A. A. S.; Ghaffarian, S. R. Synthesis and Characterization of Novel Castor Oil-Based Polyol for Potential Applications in Coatings. *J. Renewable Mater.* **2019**, *7*, 31–40.
- (3) Nagendramma, P.; Kaul, S. Development of Ecofriendly/Biodegradable Lubricants: An Overview. *Renewable Sustainable Energy Rev.* **2012**, *16*, 764–774.
- (4) Karmakar, G.; Ghosh, P.; Sharma, B. K. Chemically Modifying Vegetable Oils to Prepare Green Lubricants. *Lubricants* **2017**, *5*, No. 44.
- (5) Marques, J. P. C.; Rios, Í. C.; Parente, E. J. S.; Quintella, S. A.; Luna, F. M. T.; Cavalcante, C. L. Synthesis and Characterization of Potential Bio-Based Lubricant Basestocks via Epoxidation Process. *J. Am. Oil Chem. Soc.* **2020**, *97*, 437–446.
- (6) Wilson, B. Lubricants and Functional Fluids from Renewable Sources. *Ind. Lubr. Tribol.* **1998**, *50*, 6–15.
- (7) Sharma, B. K.; Adhvaryu, A.; Liu, Z.; Erhan, S. Z. Chemical Modification of Vegetable Oils for Lubricant Applications. *J. Am. Oil Chem. Soc.* **2006**, *83*, 129–136.
- (8) McNutt, J.; He, Q. S. Development of Biolubricants from Vegetable Oils via Chemical Modification. *J. Ind. Eng. Chem.* **2016**, *36*, 1–12.
- (9) De Laurentis, N.; Cann, P.; Lugt, P. M.; Kadircic, A. The Influence of Base Oil Properties on the Friction Behaviour of Lithium Greases in Rolling/Sliding Concentrated Contacts. *Tribol. Lett.* **2017**, *65*, No. 128.
- (10) Leveneur, S. Thermal Safety Assessment through the Concept of Structure-Reactivity: Application to Vegetable Oil Valorization. *Org. Process Res. Dev.* **2017**, *21*, 543–550.
- (11) Kurańska, M.; Beneš, H.; Prociak, A.; Trhliková, O.; Walterová, Z.; Stochlínska, W. Investigation of Epoxidation of Used Cooking Oils with Homogeneous and Heterogeneous Catalysts. *J. Cleaner Prod.* **2019**, *236*, No. 117615.
- (12) Sinadinović-Fišer, S.; Jankovi, M.; Borota, O. Epoxidation of Castor Oil with Peracetic Acid Formed in Situ in the Presence of an Ion Exchange Resin. *Chem. Eng. Process. Process Intensif.* **2012**, *62*, 106–113.
- (13) Borugadda, V. B.; Goud, V. V. Epoxidation of Castor Oil Fatty Acid Methyl Esters (COFAME) as a Lubricant Base Stock Using Heterogeneous Ion-Exchange Resin (IR-120) as a Catalyst. *Energy Procedia* **2014**, *54*, 75–84.
- (14) Isikgor, F. H.; Becer, C. R. Lignocellulosic Biomass: A Sustainable Platform for the Production of Bio-Based Chemicals and Polymers. *Polym. Chem.* **2015**, *6*, 4497–4559.
- (15) Kumar, S. Chemical modification of wood. *Wood and Fiber Science. Soc. Wood Sci. Technol.* **1994**, *26*, 270–280.
- (16) Sandberg, D.; Kutnar, A.; Mantanis, G. Wood Modification Technologies - A Review. *iForest - Biogeosciences For.* **2017**, *10*, 895–908.
- (17) Hill, C. *Wood Modifications: Chemical, Thermal, and Other Processes*; John Wiley & Sons, Ltd., 2006.
- (18) De Quadros Melo, D.; De Oliveira Sousa Neto, V.; De Freitas Barros, F. C.; Raulino, G. S. C.; Vidal, C. B.; Do Nascimento, R. F. Chemical Modifications of Lignocellulosic Materials and Their Application for Removal of Cations and Anions from Aqueous Solutions. *J. Appl. Polym. Sci.* **2016**, *133*, 1–22.
- (19) Cortés-Triviño, E.; Valencia, C.; Franco, J. M. Influence of Epoxidation Conditions on the Rheological Properties of Gel-like Dispersions of Epoxidized Kraft Lignin in Castor Oil. *Holzforchung* **2017**, *71*, 777–784.
- (20) Cortés-Triviño, E.; Valencia, C.; Delgado, M. A.; Franco, J. M. Rheology of Epoxidized Cellulose Pulp Gel-like Dispersions in Castor Oil: Influence of Epoxidation Degree and the Epoxide Chemical Structure. *Carbohydr. Polym.* **2018**, *199*, 563–571.



- (21) Jin, F.-L.; Zhang, H.; Yao, S.-S.; Park, S.-J. Mechanical and Electrical Properties of Epoxy Resin/ Epoxidized Castor Oil/Carbon Fiber Cloth Composites. *Carbon Lett.* **2017**, *22*, 105–109.
- (22) Omonov, T. S.; Kharraz, E.; Curtis, J. M. The Epoxidation of Canola Oil and Its Derivatives. *RSC Adv.* **2016**, *6*, 92874–92886.
- (23) Balan, C.; Franco, J. M. Influence of the Geometry on the Transient and Steady Flow of Lubricating Greases. *Tribol. Trans.* **2001**, *44*, 53–58.
- (24) Milchert, E.; Malarczyk-matusiak, K.; Musik, M. In *Technological Aspects of Vegetable Oils Epoxidation in the Presence of Ion Exchange Resins: A Review*, Polish Journal of Chemical Technology: A Publication of the Permanent Committee of the Polish Congresses on Chemical Technology, Vol. 18 (3), 2016; pp 128–133.
- (25) Noor Armylisas, A. H.; Siti Hazirah, M. F.; Yeong, S. K.; Hazimah, A. H. Modification of Olefinic Double Bonds of Unsaturated Fatty Acids and Other Vegetable Oil Derivatives via Epoxidation: A Review. *Grasas Aceites* **2016**, *68*, No. 174.
- (26) Sudha, G. S.; Kalita, H.; Mohanty, S.; Nayak, S. K. Biobased Epoxy Blends from Epoxidized Castor Oil: Effect on Mechanical, Thermal, and Morphological Properties. *Macromol. Res.* **2017**, *25*, 420–430.
- (27) Parada Hernandez, N. L.; Bonon, A. J.; Bahú, J. O.; Barbosa, M. I. R.; Wolf Maciel, M. R.; Filho, R. M. Epoxy Monomers Obtained from Castor Oil Using a Toxicity-Free Catalytic System. *J. Mol. Catal. A: Chem.* **2017**, *426*, 550–556.
- (28) Kyropoulos, S. On the Viscosity of Nonpolar Liquids. *J. Chem. Phys.* **1939**, *7*, 52–57.
- (29) Doll, K. M.; Cermak, S. C.; Kenar, J. A.; Walter, E. L.; Isbell, T. A. Derivatization of Castor Oil Based Estolide Esters: Preparation of Epoxides and Cyclic Carbonates. *Ind. Crops Prod.* **2017**, *104*, 269–277.
- (30) Samidin, S.; Salih, N.; Salimon, J. Synthesis and Characterization of Trimethylolpropane Based Esters as Green Biolubricant Basestock. *Biointerface Res. Appl. Chem.* **2021**, *11*, 13638–13651.
- (31) Paul, A. K.; Borugadda, V. B.; Goud, V. V. In-Situ Epoxidation of Waste Cooking Oil and Its Methyl Esters for Lubricant Applications: Characterization and Rheology. *Lubricants* **2021**, *9*, 1–14.
- (32) Rios, Í. C.; Cordeiro, J. P.; Arruda, T. B. M. G.; Rodrigues, F. E. A.; Uchoa, A. F. J.; Luna, F. M. T.; Cavalcante, C. L.; Ricardo, N. M. P. S. Chemical Modification of Castor Oil Fatty Acids (*Ricinus communis*) for Biolubricant Applications: An Alternative for Brazil's Green Market. *Ind. Crops Prod.* **2020**, *145*, No. 112000.
- (33) Lu, L.; Liu, X.; Tong, Z. Critical Exponents for Sol–Gel Transition in Aqueous Alginate Solutions Induced by Cupric Cations. *Carbohydr. Polym.* **2006**, *65*, 544–551.
- (34) Majeste, J. C.; Montfort, J. P.; Allal, A.; Marin, G. Viscoelasticity of Low Molecular Weight Polymers and the Transition to the Entangled Regime. *Rheol. Acta* **1998**, *37*, 486–499.
- (35) Cross, M. M. Rheology of Non-Newtonian Fluids: A New Flow Equation for Pseudoplastic Systems. *J. Colloid Sci.* **1965**, *20*, 417–437.
- (36) Al-Zahrani, S. M. A Generalized Rheological Model for Shear Thinning Fluids. *J. Pet. Sci. Eng.* **1997**, *17*, 211–215.
- (37) Soleymanpour, Z.; Nikzad, M.; Talebnia, F.; Niknezhad, V. Xanthan Gum Production from Acid Hydrolyzed Broomcorn Stem as a Sole Carbon Source by *Xanthomonas campestris*. *3 Biotech* **2018**, *8*, 1–12.
- (38) Neira-Velázquez, M. G.; Rodríguez-Hernández, M. T.; Hernández-Hernández, E.; Ruiz-Martínez, A. R. Y. Polymer Molecular Weight Measurement. *Handbook of Polymer Synthesis, Characterization, and Processing*; Wiley, 2013; Vol. 17, pp 355–366.
- (39) Huggins, M. L. The Viscosity of Dilute Solutions of Long-Chain Molecules. I. *J. Phys. Chem. A* **1938**, *42*, 911–920.
- (40) Kamli, M.; Guettari, M.; Tajouri, T. Structure of Polyvinylpyrrolidone Aqueous Solution in Semi-Dilute Regime: Roles of Polymer-Surfactant Complexation. *J. Mol. Struct.* **2019**, *1196*, 176–185.
- (41) Mary, C.; Philippon, D.; Lafarge, L.; Laurent, D.; Rondelez, F.; Bair, S.; Vergne, P. New Insight into the Relationship between Molecular Effects and the Rheological Behavior of Polymer-Thickened Lubricants under High Pressure. *Tribol. Lett.* **2013**, *52*, 357–369.
- (42) Bercea, M.; Gradinaru, L. M.; Mandru, M.; Tigau, D. L.; Ciobanu, C. Intermolecular Interactions and Self-Assembling of Polyurethane with Poly(Vinyl Alcohol) in Aqueous Solutions. *J. Mol. Liq.* **2019**, *274*, 562–567.
- (43) Wolf, B. A. Polyelectrolytes Revisited: Reliable Determination of Intrinsic Viscosities. *Macromol. Rapid Commun.* **2007**, *28*, 164–170.
- (44) Eckelt, J.; Knopf, A.; Wolf, B. A. Polyelectrolytes: Intrinsic Viscosities in the Absence and in the Presence of Salt. *Macromolecules* **2008**, *41*, 912–918.
- (45) da Costa, M. P. M.; Delpech, M. C.; de Mello Ferreira, I. L.; de Macedo Cruz, M. T.; Castanharo, J. A.; Cruz, M. D. Evaluation of Single-Point Equations to Determine Intrinsic Viscosity of Sodium Alginate and Chitosan with High Deacetylation Degree. *Polym. Test.* **2017**, *63*, 427–433.
- (46) Dallmeyer, I.; Ko, F.; Kadla, J. F. Electrospinning of Technical Lignins for the Production of Fibrous Networks. *J. Wood Chem. Technol.* **2010**, *30*, 315–329.
- (47) Dodero, A.; Vicini, S.; Alloisio, M.; Castellano, M. Sodium Alginate Solutions: Correlation between Rheological Properties and Spinnability. *J. Mater. Sci.* **2019**, *54*, 8034–8046.
- (48) Liu, Y.; Jun, Y.; Steinberg, V. Concentration Dependence of the Longest Relaxation Times of Dilute and Semi-Dilute Polymer Solutions. *J. Rheol.* **2009**, *53*, 1069. DOI: 10.1122/1.3160734.
- (49) Lopez, C. G.; Richtering, W. Influence of Divalent Counterions on the Solution Rheology and Supramolecular Aggregation of Carboxymethyl Cellulose. *Cellulose* **2018**, *26*, 1517–1534.
- (50) Magda, J. J.; Baekt, S. G. Concentrated Entangled and Semidilute Entangled Polystyrene Solutions and the Second Normal Stress Difference. *Polymer* **1994**, *35*, 1187–1194. DOI: 10.1016/0032-3861(94)90010-8.
- (51) Van Krevelen, D. W.; Te Nijenhuis, K. *Properties of Polymers*; Elsevier, 2009.
- (52) Kremer, F.; Lagaly, G. *Progress in Colloid and Polymer Science*; Springer, 1999; Vol. 113.
- (53) Cousins, D. S.; Tan, B.; Howell, J.; Suzuki, Y.; Samaniuk, J. R.; Knauss, D. M.; Dorgan, J. R. Styrene-Free, Partially Biobased Resin System for Thermoplastic Composites. I. Rheological Properties and Preliminary Panel Fabrication. *ACS Sustainable Chem. Eng.* **2019**, *7*, 6512–6521.
- (54) Masuelli, M. A. Viscometric Study of Pectin. Effect of Temperature on the Hydrodynamic Properties. *Int. J. Biol. Macromol.* **2011**, *48*, 286–291.
- (55) Karmanov, A. P.; Kocheva, L. S. Study of the Topological Structure of *Bamboo bambusa* Sp. Lignin Macromolecules. *Polym. Sci., Ser. A* **2018**, *60*, 464–470.
- (56) Dong, D.; Fricke, A. L. Intrinsic Viscosity and the Molecular Weight of Kraft Lignin. *Polymer* **1995**, *36*, 2075–2078.
- (57) Glasser, W. G.; Davé, V.; Frazier, C. E. Molecular Weight Distribution of (Semi-) Commercial Lignin Derivatives. *J. Wood Chem. Technol.* **1993**, *13*, 545–559.
- (58) Wang, L.; Uraki, Y.; Koda, K.; Gele, A.; Zhou, X.; Chen, F. Determination of the Absolute Molar Mass of Acetylated Eucalyptus Kraft Lignin by Two Types of Size-Exclusion Chromatography Combined with Multi-Angle Laser Light-Scattering Detectors. *Holzforchung* **2019**, *73*, 363–369.
- (59) Masuelli, M. A. Mark-Houwink Parameters for Aqueous-Soluble Polymers and Biopolymers at Various Temperatures. *J. Polym. Biopolym. Phys. Chem.* **2014**, *2*, 37–43.
- (60) Karmanov, A. P.; Kocheva, L. S. Study of the Structure of Lignin Macromolecules by Molecular Hydrodynamics Methods. *Russ. Chem. Bull.* **2014**, *63*, 2040–2044.
- (61) Tosh, B. N.; Saikia, C. N. Mark-Houwink-Sakurada Constants for Cellulose-Paraformaldehyde/Dimethyl Sulphoxide System. *Indian J. Chem. Technol.* **1997**, *4*, 247–250.

(62) Kasaai, M. R. Comparison of Various Solvents for Determination of Intrinsic Viscosity and Viscometric Constants for Cellulose. *J. Appl. Polym. Sci.* **2002**, *86*, 2189–2193.

(63) Ringena, O.; Lebioda, S.; Lehnen, R.; Saake, B. Size-Exclusion Chromatography of Technical Lignins in Dimethyl Sulfoxide/Water and Dimethylacetamide. *J. Chromatogr. A* **2006**, *1102*, 154–163.

(64) Glasser, W. G.; Jain, R. K. Lignin Derivatives. *Holzforschung* **1993**, *47*, 225–233.

(65) Zeng, J.; Tong, Z.; Wang, L.; Zhu, J. Y.; Ingram, L. Isolation and Structural Characterization of Sugarcane Bagasse Lignin after Dilute Phosphoric Acid plus Steam Explosion Pretreatment and Its Effect on Cellulose Hydrolysis. *Bioresour. Technol.* **2014**, *154*, 274–281.

(66) Bezerra, T. L.; Ragauskas, A. J. A Review of Sugarcane Bagasse for Second-Generation Bioethanol and Biopower Production. *Biofuels, Bioprod. Biorefin.* **2016**, *10*, 634–647.